First Evidence of *pep* Solar Neutrinos by Direct Detection in Borexino

G. Bellini,[1] J. Benziger,[2] D. Bick,[3] S. Bonetti,[1] G. Bonfini,[4] D. Bravo,[5] M. Buizza Avanzini,[1] B. Caccianiga,[1] L. Cadonati,[6] F. Calaprice,[7] C. Carraro,[8] P. Cavalcante,[4] A. Chavarria,[7] A. Chepurnov,[9] D. D'Angelo,[1] S. Davini,[8,10] A. Derbin,[11] A. Etenko,[12] K. Fomenko,[13,4] D. Franco,[14] C. Galbiati,[7] S. Gazzana,[4] C. Ghiano,[4] M. Giammarchi,[1] M. Goeger-Neff,[15] A. Goretti,[7] L. Grandi,[7] E. Guardincerri,[8] S. Hardy,[5] Aldo Ianni,[4] Andrea Ianni,[7] D. Korablev,[13] G. Korga,[4,10] Y. Koshio,[4] D. Kryn,[14] M. Laubenstein,[4] T. Lewke,[15] E. Litvinovich,[12] B. Loer,[7] F. Lombardi,[4] P. Lombardi,[1] L. Ludhova,[1] I. Machulin,[12] S. Manecki,[5] W. Maneschg,[16] G. Manuzio,[8] Q. Meindl,[15] E. Meroni,[1] L. Miramonti,[1] M. Misiaszek,[17,4] D. Montanari,[4,7] P. Mosteiro,[7] V. Muratova,[11] L. Oberauer,[15] M. Obolensky,[14] F. Ortica,[18] K. Otis,[6] M. Pallavicini,[8] L. Papp,[5] L. Perasso,[8] S. Perasso,[8] A. Pocar,[6] J. Quirk,[6] R. S. Raghavan,[5] G. Ranucci,[1] A. Razeto,[4] A. Re,[1] A. Romani,[18] A. Sabelnikov,[12] R. Saldanha,[7] C. Salvo,[8] S. Schönert,[15] H. Simgen,[16] M. Skorokhvatov,[12] O. Smirnov,[13] A. Sotnikov,[13] S. Sukhotin,[12] Y. Suvorov,[4,19] R. Tartaglia,[4] G. Testera,[8] D. Vignaud,[14] R. B. Vogelaar,[5] F. von Feilitzsch,[15] J. Winter,[15] M. Wojcik,[17] A. Wright,[7] M. Wurm,[3] J. Xu,[7] O. Zaimidoroga,[13] S. Zavatarelli,[8] and G. Zuzel[17]

(Borexino Collaboration)

[1]*Dipartimento di Fisica, Università degli Studi e INFN, 20133 Milano, Italy*
[2]*Chemical Engineering Department, Princeton University, Princeton, New Jersey 08544, USA*
[3]*Institut für Experimentalphysik, Universität, 22761 Hamburg, Germany*
[4]*INFN Laboratori Nazionali del Gran Sasso, SS 17 bis Km 18+910, 67010 Assergi, Italy*
[5]*Physics Department, Virginia Polytechnic Institute and State University, Blacksburg, Virginia 24061, USA*
[6]*Physics Department, University of Massachusetts, Amherst, Massachusetts 01003, USA*
[7]*Physics Department, Princeton University, Princeton, New Jersey 08544, USA*
[8]*Dipartimento di Fisica, Università e INFN, Genova 16146, Italy*
[9]*Physics Department, Lomonosov Moscow State University, Moscow 119991, Russia*
[10]*Physics Department, University of Houston, Houston, Texas 77204, USA*
[11]*St. Petersburg Nuclear Physics Institute, 188350 Gatchina, Russia*
[12]*NRC Kurchatov Institute, 123182 Moscow, Russia*
[13]*Joint Institute for Nuclear Research, 141980 Dubna, Russia*
[14]*Laboratoire AstroParticule et Cosmologie, 75205 Paris cedex 13, France*
[15]*Physik Department, Technische Universität München, 85747 Garching, Germany*
[16]*Max-Planck-Institut für Kernphysik, 69117 Heidelberg, Germany*
[17]*M. Smoluchowski Institute of Physics, Jagiellonian University, 30059 Krakow, Poland*
[18]*Dipartimento di Chimica, Università e INFN, 06123 Perugia, Italy*
[19]*Physics and Astronomy Department, University of California at Los Angeles, Los Angeles, California, 90095, USA*

(Received 14 October 2011; published 2 February 2012)

We observed, for the first time, solar neutrinos in the 1.0–1.5 MeV energy range. We determined the rate of *pep* solar neutrino interactions in Borexino to be $3.1 \pm 0.6_{\mathrm{stat}} \pm 0.3_{\mathrm{syst}}$ counts/(day · 100 ton). Assuming the *pep* neutrino flux predicted by the standard solar model, we obtained a constraint on the CNO solar neutrino interaction rate of <7.9 counts/(day · 100 ton) (95% C.L.). The absence of the solar neutrino signal is disfavored at 99.97% C.L., while the absence of the *pep* signal is disfavored at 98% C.L. The necessary sensitivity was achieved by adopting data analysis techniques for the rejection of cosmogenic ^{11}C, the dominant background in the 1–2 MeV region. Assuming the Mikheyev-Smirnov-Wolfenstein large mixing angle solution to solar neutrino oscillations, these values correspond to solar neutrino fluxes of $(1.6 \pm 0.3) \times 10^8$ cm^{-2} s^{-1} and $<7.7 \times 10^8$ cm^{-2} s^{-1} (95% C.L.), respectively, in agreement with both the high and low metallicity standard solar models. These results represent the first direct evidence of the *pep* neutrino signal and the strongest constraint of the CNO solar neutrino flux to date.

DOI: 10.1103/PhysRevLett.108.051302 PACS numbers: 26.65.+t, 14.60.Lm, 95.55.Vj, 97.20.Jg

Over the past 40 years, solar neutrino (ν) experiments [1–5] have proven to be sensitive tools to test both astrophysical and elementary particle physics models. Solar neutrino detectors have demonstrated that stars are powered by nuclear fusion reactions. Two distinct processes, the main *pp* fusion chain and the subdominant CNO cycle, are expected to produce solar ν_e with different energy spectra and fluxes. Until now, only fluxes from the *pp*

 © 2012 American Physical Society

chain have been measured: ^{7}Be, ^{8}B, and, indirectly, pp. Experiments involving solar ν and reactor $\bar{\nu}_e$ [6] have shown that solar ν_e undergo flavor oscillations.

Results from solar-ν experiments are consistent with the Mikheyev-Smirnov-Wolfenstein large mixing angle (MSW-LMA) model [7], which predicts a transition from vacuum-dominated to matter-enhanced oscillations, resulting in an energy-dependent ν_e survival probability, P_{ee}. Nonstandard neutrino interaction models formulate P_{ee} curves that deviate significantly from MSW-LMA, particularly in the 1–4 MeV transition region; see, e.g., [8]. The monoenergetic 1.44 MeV pep neutrinos, which belong to the pp chain and whose standard solar model (SSM) predicted flux has one of the smallest uncertainties (1.2%) due to the solar luminosity constraint [9], are an ideal probe to test these competing hypotheses.

The detection of neutrinos resulting from the CNO cycle has important implications in astrophysics, as it would be the first direct evidence of the nuclear process that is believed to fuel massive stars ($> 1.5 M_{\odot}$). Furthermore, its measurement may help to resolve the solar metallicity problem [9,10]. The energy spectrum of neutrinos from the CNO cycle is the sum of three continuous spectra with end point energies of 1.19 (^{13}N), 1.73 (^{15}O), and 1.74 MeV (^{17}F), close to the pep ν energy. The total CNO ν flux is similar to that of the pep ν, but its predicted value is strongly dependent on the inputs to the solar modeling, being 40% higher in the high metallicity (GS98) than in the low metallicity (AGSS09) solar model [9].

Neutrinos interact through elastic scattering with electrons (e^-) in the ~278 ton organic liquid scintillator target of Borexino [11]. The e^- recoil energy spectrum from pep neutrino interactions in Borexino is a Compton-like shoulder with an end point of 1.22 MeV. High light yield and low background levels [5,12] allow Borexino to perform solar-ν spectroscopy below 2 MeV. Its potential has already been demonstrated in the precision measurement of the 0.862 MeV ^{7}Be solar-ν flux [5,13]. The detection of pep and CNO neutrinos requires new analysis techniques, as their expected interaction rates are a few counts per day in a 100 ton target.

We adopted analysis procedures to suppress the dominant background in the 1–2 MeV energy range, the cosmogenic β^+ emitter ^{11}C (lifetime: 29.4 min). ^{11}C is produced in the scintillator by cosmic muon (μ) interactions with ^{12}C nuclei. The muon flux through Borexino is ~4300 μ/day, yielding a ^{11}C production rate of ~27 counts/(day · 100 ton). In 95% of the cases, at least one free neutron is spalled in the ^{11}C production process [14] and then captured in the scintillator with a mean time of 255 μs [15]. The ^{11}C background can be reduced by performing a space and time veto after coincidences between signals from the muons and the cosmogenic neutrons [16,17], discarding exposure that is more likely to contain ^{11}C due to the correlation between the parent μ, the neutron, and the subsequent ^{11}C decay (the threefold coincidence, TFC). The technique relies on the reconstructed track of the μ and the reconstructed position of the neutron-capture γ ray [15]. We have applied different veto configurations on the data, resulting in different residual ^{11}C rates and exposures. From an analysis on simulated data samples, we estimated which configuration leads to the smallest expected uncertainty in the neutrino interaction rates. The best veto criteria result in a ^{11}C rate of (2.5 ± 0.3) counts/(day · 100 ton), (9 ± 1)% of the original rate, while preserving 48.5% of the initial exposure. The resulting spectrum (Fig. 1, top) corresponds to a fiducial exposure of 20 409 ton · day, consisting of data collected between January 13, 2008, and May 9, 2010.

The ^{11}C surviving the TFC veto is still a significant background. We exploited the pulse-shape differences between e^- and e^+ interactions in organic liquid scintillators

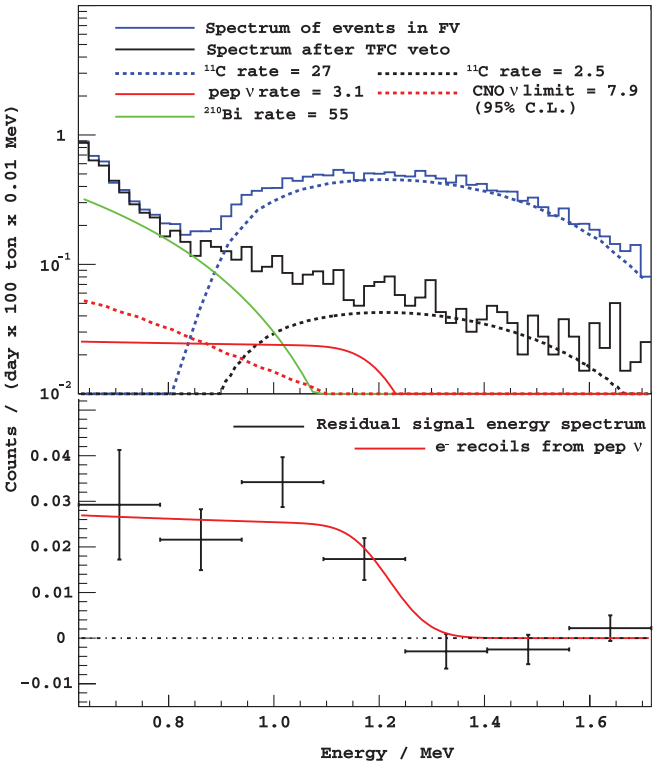

FIG. 1 (color). Top: energy spectra of the events in the FV before and after the TFC veto is applied. The solid and dashed blue lines show the data and estimated ^{11}C rate before any veto is applied. The solid black line shows the data after the procedure, in which the ^{11}C contribution (dashed black line) has been greatly suppressed. The next largest background, ^{210}Bi, and the e^- recoil spectra of the best estimate of the pep-ν rate and of the upper limit of the CNO-ν rate are shown for reference. Rate values in the legend are integrated over all energies and are quoted in units of counts/(day · 100 metric ton). Bottom: residual energy spectrum after best-fit rates of all considered backgrounds are subtracted. The e^- recoil spectrum from pep-ν at the best-fit rate is shown for comparison.

[18] to discriminate ^{11}C β^+ decays from neutrino-induced e^- recoils and β^- decays [19].

A slight difference in the time distribution of the scintillation signal arises from the finite lifetime of ortho-positronium, as well as from the presence of annihilation γ rays, which present a distributed, multisite event topology and a larger average ionization density than e^- interactions. An optimized pulse-shape parameter was constructed using a boosted-decision-tree algorithm [20], trained with a TFC-selected set of ^{11}C events (e^+) and ^{214}Bi events (e^-) selected by the fast ^{214}Bi-^{214}Po α-β decay sequence.

We present results of an analysis based on a binned likelihood multivariate fit performed on the energy, pulse shape, and spatial distributions of selected scintillation events whose reconstructed position is within the fiducial volume (FV), i.e., less than 2.8 m from the detector center and with a vertical position relative to the detector center between -1.8 m and 2.2 m. As in previous work [5], we used two distinct approaches for modeling the detector energy response, one which is Monte Carlo-based and one which is based on an analytic description. We confirmed the accuracy of the modeling in both cases by means of an extensive calibration campaign with α, β, γ, and neutron sources deployed within the active target [5].

The distribution of the pulse-shape parameter (Fig. 2) was a key element in the multivariate fit, where decays from cosmogenic ^{11}C (and ^{10}C) were considered e^+ and all other species e^-.

The energy spectra and spatial distribution of the external γ-ray backgrounds have been obtained from a full, GEANT4-based Monte Carlo simulation, starting with the radioactive decays of contaminants in the detector peripheral structure and propagating the particles into the active volume. We validated the simulation with calibration data from a high-activity ^{228}Th source [21] deployed in the outermost buffer region, outside the active volume. The nonuniform radial distribution of the external background was included in the multivariate fit and strongly constrained its contribution. Internal radioactive backgrounds and e^- recoils from solar ν were assumed to be uniformly distributed. Figure 3 shows the radial component of the fit.

We removed α events from the energy spectrum by the method of statistical subtraction [5]. The species left free in the fit were the internal radioactive backgrounds ^{210}Bi, ^{40}K, ^{85}Kr, and ^{234m}Pa (from the ^{238}U decay chain); the cosmogenic backgrounds ^{11}C, ^{10}C, and ^{6}He; the e^- recoils from ^{7}Be, pep, and CNO solar ν; and the external γ rays from ^{208}Tl, ^{214}Bi, and ^{40}K. The rates of all these species were constrained to positive values. We fixed the contribution from pp and ^{8}B solar ν, respectively, to the SSM predicted rate (assuming MSW-LMA with $\tan^2\theta_{12} = 0.47^{+0.05}_{-0.04}$, $\Delta m^2_{12} = (7.6 \pm 0.2) \times 10^{-5}$ eV^2 [22]) and to the rate from the measured flux [4]. We fixed the rate of the radon daughter ^{214}Pb using the measured rate of ^{214}Bi-^{214}Po delayed coincidence events.

Simultaneously to the fit of events surviving the TFC veto, we also fit the energy spectrum of events rejected by the veto, corresponding to the remaining 51.5% of the exposure. We constrained the rate for every noncosmogenic species to be the same in both data sets, since only cosmogenic isotopes are expected to be correlated with neutron production.

Fits to simulated event distributions, under the same configuration as the fit to real data, including the same species, variables, and constraints, returned results for the pep and CNO neutrino interaction rates that were unbiased. These tests also yielded the distributions of the resulting best-fit likelihood values, from which we confirmed the validity of the likelihood ratio test used to

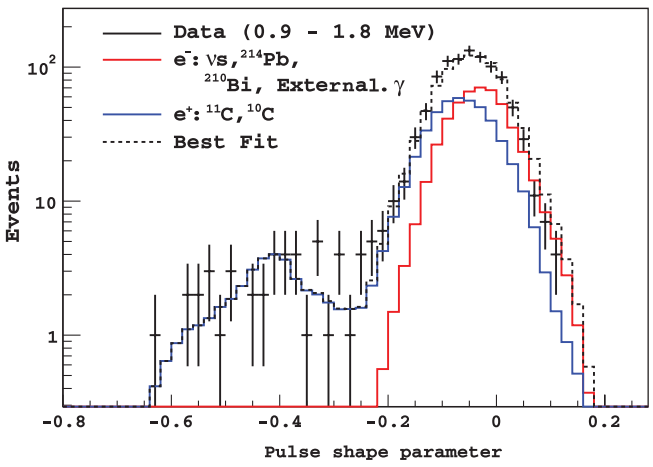

FIG. 2 (color). Experimental distribution of the pulse-shape parameter (black data points). The best-fit distribution (dashed black line) and the corresponding e^- (solid red line) and e^+ (solid blue line) contributions are also shown.

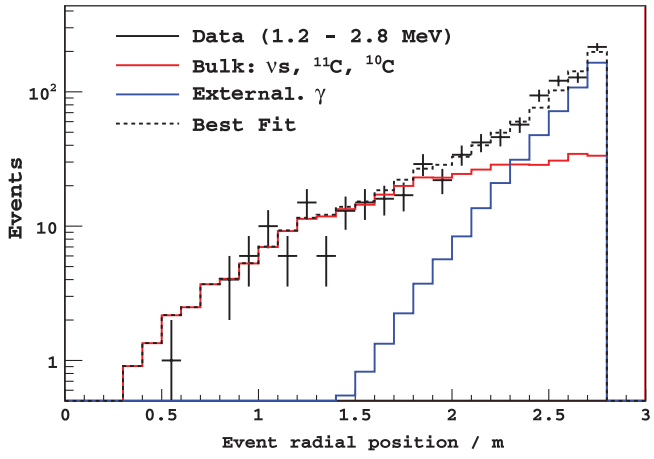

FIG. 3 (color). Experimental distribution of the radial coordinate of the reconstructed position within the FV (black data points). The best-fit distribution (dashed black line) and the corresponding contributions from bulk events (solid red line) and external γ rays (solid blue line) are also shown.

TABLE I. The best estimates for the *pep* and CNO solar neutrino interaction rates. The statistical uncertainties are not Gaussian, as can be seen in Fig. 4. For the results in the last two columns, both statistical and systematic uncertainties are considered. Total fluxes have been obtained assuming MSW-LMA and using the scattering cross sections from [22–24] and a scintillator e^- density of $(3.307 \pm 0.003) \times 10^{29}$ ton^{-1}. The last column gives the ratio between our measurement and the high metallicity (GS98) SSM [9].

ν	Interaction rate [counts/(day · 100 ton)]	Solar-ν flux [10^8 cm^{-2} s^{-1}]	Data/SSM ratio
pep	$3.1 \pm 0.6_{\text{stat}} \pm 0.3_{\text{syst}}$	1.6 ± 0.3	1.1 ± 0.2
CNO	<7.9 ($<7.1_{\text{stat only}}$)	<7.7	<1.5

compute uncertainties and limits, and determined the p value of our best fit to the real data to be 0.3. Table I summarizes the results for the *pep* and CNO neutrino interaction rates. The absence of the solar-ν signal was rejected at 99.97% C.L., using a likelihood ratio test between the result when the *pep* and CNO neutrino interaction rates were fixed to zero and the best-fit result. Likewise, the absence of a *pep* ν signal was rejected at 98% C.L. Because of the similarity between the e^- recoil spectrum from CNO neutrinos and the spectral shape of ^{210}Bi decay, whose rate is ~10 times greater, we can only provide an upper limit on the CNO ν interaction rate. The 95% C.L. limit reported in Table I has been obtained from a likelihood ratio test with the *pep* ν rate fixed to the SSM prediction [9] under the assumption of MSW-LMA, (2.80 ± 0.04) counts/(day · 100 ton), which leads to the strongest test of the solar metallicity. For reference, Fig. 4 shows the full $\Delta\chi^2$ profile for *pep* and CNO neutrino interaction rates.

The estimated ^{7}Be ν interaction rate is consistent with our measurement [5]. Table II summarizes the estimates for the rates of the other background species. The higher rate of ^{210}Bi decays compared to [5] is due to the exclusion of data from 2007, when the observed decay rate of ^{210}Bi in the FV was smallest. The correlation of this background with detector fluid operations has confirmed that its source is permanent radioactive contamination in the scintillator (^{210}Pb).

Table III shows the relevant sources of systematic uncertainty. The uncertainty associated with the detector energy response has been estimated by performing fits using different reference spectra, modified according to the uncertainty in the detector response function. To evaluate the uncertainty associated with the fit methods, we have performed fits changing the binning of the energy spectra, the fit range, and the energy bins for which the radial and pulse-shape parameter distributions were fit. We consider the results of both approaches for the modeling of the detector energy response. The impact of the limited statics in the reference pulse-shape distributions has been determined by performing fits where their bin content was randomly modified according to Poisson statistics.

Further systematic checks that offer a negligible contribution to the total uncertainty have been carried out. These include the stability of the fit over different exposure periods, the shape of the external γ ray and CNO spectra, and the fixing of ^{214}Pb in the fit. Constraining the ^{8}B and *pp* neutrino interaction rates using the measured flux and SSM values, respectively, introduces a very small systematic (changing the assumed ^{8}B ν rate by 30% induces a <1% change in the fitted *pep* ν rate); therefore, over reasonable ranges of parameter space, our result can be taken to be uncorrelated with those inputs. We have estimated that the cumulative contribution of ^{232}Th and ^{235}U daughters; other cosmogenic isotopes (^{8}He, ^{8}Li, ^{9}Li, ^{7}Be, ^{11}Be, ^{8}B, ^{12}B, and ^{9}C); neutron captures, e^+ from $\bar{\nu}_e$;

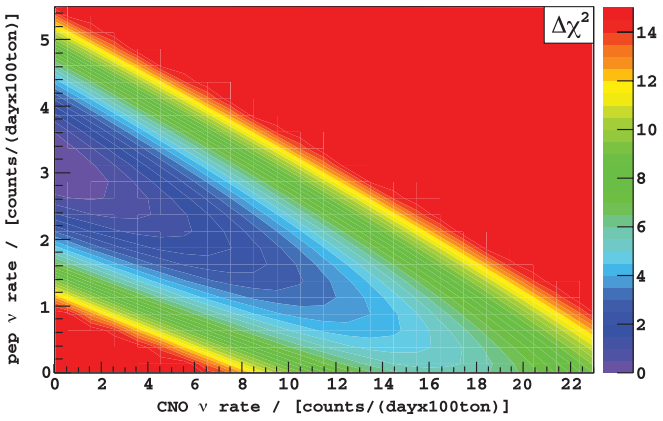

FIG. 4 (color). $\Delta\chi^2$ profile obtained from likelihood ratio tests between fit results where the *pep* and CNO neutrino interaction rates are fixed to particular values (other species are left free) and the best-fit result.

TABLE II. The best estimates for the total rates of the background species included in the fit. The statistical and systematic uncertainties were added in quadrature. The expected rates for the cosmogenic isotopes ^{11}C, ^{10}C, and ^{6}He have been obtained following the methodology outlined in [25]. The expected ^{234m}Pa rate was determined from the ^{214}Bi-^{214}Po measured coincidence rate, under the assumption of secular equilibrium. External γ includes the estimated contributions from ^{208}Tl, ^{214}Bi, and ^{40}K external γ rays.

Background	Interaction rate [counts/(day · 100 ton)]	Expected rate [counts/(day · 100 ton)]
^{85}Kr	19^{+5}_{-3}	30 ± 6 [5]
^{210}Bi	55^{+3}_{-5}	···
^{11}C	27.4 ± 0.3	28 ± 5
^{10}C	0.6 ± 0.2	0.54 ± 0.04
^{6}He	<2	0.31 ± 0.04
^{40}K	<0.4	···
^{234m}Pa	<0.5	0.57 ± 0.05
External γ	2.5 ± 0.2	···

TABLE III. Relevant sources of systematic uncertainty and their contribution in the measured *pep* neutrino interaction rate. These systematics increase the upper limit in the CNO neutrino interaction rate by 0.8 counts/(day · 100 ton).

Source	[%]
Fiducial exposure	$^{+0.6}_{-1.1}$
Energy response	± 4.1
^{210}Bi spectral shape	$^{+1.0}_{-5.0}$
Fit methods	± 5.7
Inclusion of independent ^{85}Kr estimate	$^{+3.9}_{-0.0}$
γ rays in pulse-shape distributions	± 2.7
Statistical uncertainties in pulse-shape distributions	± 5
Total systematic uncertainty	± 10

untagged muons; and pileup events decreases the central value of the *pep* ν rate by $<2\%$.

Table I also shows the solar neutrino fluxes inferred from our best estimates of the *pep* and CNO neutrino interaction rates, assuming the MSW-LMA solution, and the ratio of these values to the high metallicity (GS98) SSM predictions [9]. Both results are consistent with the predicted high and low metallicity SSM fluxes assuming MSW-LMA. Under the assumption of no neutrino flavor oscillations, we would expect a *pep* neutrino interaction rate in Borexino of (4.47 ± 0.05) counts/(day · 100 ton); the observed interaction rate disfavors this hypothesis at 97% C.L. If this discrepancy is due to ν_e oscillation to ν_μ or ν_τ, we find $P_{ee} = 0.62 \pm 0.17$ at 1.44 MeV. This result is shown alongside other solar neutrino P_{ee} measurements and the MSW-LMA prediction in Fig. 5.

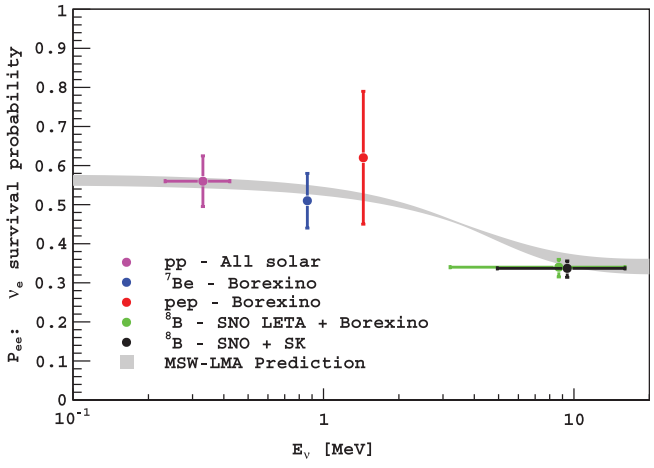

FIG. 5 (color). Electron neutrino survival probability as a function of energy. The red line corresponds to the measurement presented in this Letter. The *pp* and ^{7}Be measurements of P_{ee} given in [5] are also shown. The ^{8}B measurements of P_{ee} were obtained from [3,4,25], as indicated in the legend. The MSW-LMA prediction band is the 1σ range of the mixing parameters given in [22].

We have achieved the necessary sensitivity to provide, for the first time, evidence of the signal from *pep* neutrinos and to place the strongest constraint on the CNO neutrino flux to date. This has been made possible by the combination of low levels of intrinsic background in Borexino and the implementation of novel background discrimination techniques. The result for the *pep* ν interaction rate does not have sufficient precision to disentangle the P_{ee} predictions of various oscillation models, and the constraint on the CNO ν flux cannot yet discern between the high and low metallicity SSM. However, the success in the reduction of ^{11}C background raises the prospect for higher precision measurements of *pep* and CNO neutrino interaction rates by Borexino after further running, especially if the next dominant background, ^{210}Bi, is reduced by scintillator repurification.

The Borexino program is made possible by funding from INFN (Italy), NSF (USA), BMBF, DFG, and MPG (Germany), NRC Kurchatov Institute (Russia), and MNiSW (Poland). We acknowledge the generous support of the Gran Sasso National Laboratories (LNGS).

[1] B. T. Cleveland *et al.*, Astrophys. J. **496**, 505 (1998); K. Lande and P. Wildenhain, Nucl. Phys. B, Proc. Suppl. **118**, 49 (2003); R. Davis, Nobel Prize in Physics in 2002.

[2] F. Kaether *et al.*, Phys. Lett. B **685**, 47 (2010); W. Hampel *et al.* (GALLEX Collaboration), *ibid.* **447**, 127 (1999); J. N. Abdurashitov *et al.* (SAGE Collaboration), Phys. Rev. C **80**, 015807 (2009).

[3] K. S. Hirata *et al.* (KamiokaNDE Collaboration), Phys. Rev. Lett. **63**, 16 (1989); Y. Fukuda *et al.* (Super-Kamiokande Collaboration), *ibid.* **81**, 1562 (1998); J. P. Cravens *et al.* (Super-KamiokaNDE Collaboration), Phys. Rev. D **78**, 032002 (2008).

[4] Q. R. Ahmad *et al.* (SNO Collaboration), Phys. Rev. Lett. **87**, 071301 (2001); B. Aharmim *et al.* (SNO Collaboration), Phys. Rev. C **75**, 045502 (2007); **81**, 055504 (2010); arXiv:1109.0763v1.

[5] C. Arpesella *et al.* (Borexino Collaboration), Phys. Lett. B **658**, 101 (2008); Phys. Rev. Lett. **101**, 091302 (2008); G. Bellini *et al.* (Borexino Collaboration), *ibid.* **107**, 141302 (2011).

[6] S. Abe *et al.* (KamLAND Collaboration), Phys. Rev. Lett. **100**, 221803 (2008).

[7] S. P. Mikheyev and A. Yu. Smirnov, Sov. J. Nucl. Phys. **42**, 913 (1985); L. Wolfenstein, Phys. Rev. D **17**, 2369 (1978); P. C. de Holanda and A. Yu. Smirnov, J. Cosmol. Astropart. Phys. 02 (2003) 001.

[8] A. Friedland *et al.*, Phys. Lett. B **594**, 347 (2004); S. Davidson *et al.*, J. High Energy Phys. 03 (2003) 011; P. C. de Holanda and A. Yu. Smirnov, Phys. Rev. D **69**, 113002 (2004); A. Palazzo and J. W. F. Valle, *ibid.* **80**, 091301 (2009).

[9] A. M. Serenelli, W. C. Haxton, and C. Peña-Garay, Astrophys. J. **743**, 24 (2011).

[10] S. Basu, Astron. Soc. Pac. Conf. Ser. **416**, 193 (2009).

[11] G. Alimonti *et al.* (Borexino Collaboration), Nucl. Instrum. Methods Phys. Res., Sect. A **600**, 568 (2009).
[12] G. Alimonti *et al.* (Borexino Collaboration), Nucl. Instrum. Methods Phys. Res., Sect. A **609**, 58 (2009).
[13] G. Bellini *et al.* (Borexino Collaboration), Phys. Lett. B **707**, 22 (2012).
[14] C. Galbiati, A. Pocar, D. Franco, A. Ianni, L. Cadonati, and S. Schönert, Phys. Rev. C **71**, 055805 (2005).
[15] G. Bellini *et al.* (Borexino Collaboration), JINST **6**, P05005 (2011).
[16] M. Deutsch, *Proposal for a Cosmic Ray Detection System for the Borexino Solar Neutrino Experiment* (Massachusetts Institute of Technology, Cambridge, MA, 1996).
[17] H. Back *et al.* (Borexino Collaboration), Phys. Rev. C **74**, 045805 (2006).
[18] Y. Kino *et al.*, J. Nucl. Radiochem. Sci. **1**, 63 (2000).
[19] D. Franco, G. Consolati, and D. Trezzi, Phys. Rev. C **83**, 015504 (2011).
[20] TMVA Users Guide, http://tmva.sourceforge.net/docu/TMVAUsersGuide.pdf.
[21] W. Maneschg *et al.*, arXiv:1110.1217.
[22] K. Nakamura *et al.* (Particle Data Group), J. Phys. G **37**, 075021 (2010).
[23] J. N. Bahcall, M. Kamionkowski, and A. Sirlin, Phys. Rev. D **51**, 6146 (1995).
[24] J. Erler and M. J. Ramsey-Musolf, Phys. Rev. D **72**, 073003 (2005).
[25] G. Bellini *et al.* (Borexino Collaboration), Phys. Rev. D **82**, 033006 (2010).